Available online at www.sciencedirect.com

ScienceDirect

Ceramics International 41 (2015) 755–760

CERAMICS INTERNATIONAL

www.elsevier.com/locate/ceramint

Combustion synthesis of lead oxide nanopowders for the preparation of PMN–PT transparent ceramics

Xuan Chen[a,b], Shi Chen[b,*], Pierre-Marie Clequin[b], William T. Shoulders[a,b], Romain Gaume[a,b,c,*]

[a]Department of Materials Science and Engineering, University of Central Florida, Orlando, FL 32816, USA
[b]College of Optics and Photonics, University of Central Florida, Orlando, FL 32816, USA
[c]NanoScience Technology Center, University of Central Florida, Orlando, FL 32816, USA

Received 23 July 2014; received in revised form 20 August 2014; accepted 1 September 2014
Available online 6 September 2014

Abstract

We describe the preparation of lead oxide nanopowders by a combustion synthesis process in which nitric acid and glycine are used as oxidant and fuel reagents respectively. We observe that the fuel-to-oxidant ratio affects the phase formation, valence, yield, particle shape and size of lead oxide powders. 60 nm-diameter lead oxide particles, with a yield of 86%, were obtained for a 1.7 glycine-to-nitrate molar ratio. This process produces powders with greater uniformity and smaller particle size than commercially available and we illustrate the improvement that these nanopowders offer in the synthesis of $(1-x)Pb(Mg_{1/3}Nb_{2/3})O_3$–$xPbTiO_3$ (called PMN–PT) transparent ceramics by solid-state reaction.

Keywords: PMN–PT; Glycine–nitrate process; Lead oxide nanopowders; Combustion synthesis

1. Introduction

Despite current efforts to limit the use of heavy metals in technological applications, lead oxide powders are still important precursors in the synthesis of a variety of materials including flint glass, phosphors [1], materials for gas sensing [2], data [3] and energy storage [4]. In particular, lead-based transparent ferroelectrics are significant optoelectronics materials [5–7] which exhibit extremely high electro-optic coefficients and strong photorefractive effects [8,9]. One of the most representative material of this class, $(1-x)Pb(Mg_{1/3}Nb_{2/3})O_3$–$xPbTiO_3$ or PMN–PT, also presents large non-linear susceptibility coefficients and is therefore attractive in nonlinear optical applications. Current efforts aim at developing reliable PMN–PT fabrication methods to improve on the optical clarity and optical damage threshold [10]. Compared to single-crystals which are difficult to grow for these compositions [11], ceramics can be easily hot-pressed or sintered in a variety of sizes and shapes with a high degree of optical uniformity on a macroscopic scale. Soft mechanochemical pulverization [12], sol–gel method [13], chemical co-precipitation method [14], B-site precursor method [15] have been reported for synthesis of PMN–PT ceramics. Conventionally, PMN–PT powder has been synthesized by the solid-state mixed oxides method [16–18]. One of the main challenges associated to the fabrication of high-quality PMN–PT is the avoidance of a parasitic pyrochlore phase ($A_2B_2O_7$, A and B metals), which not only decreases the dielectric and piezoelectric properties of the materials [19], but also degrades the optical transmission by introducing scattering centers [20]. The formation of pyrochlore (also observed in bismuth-containing ferroelectric compounds) is attributed to the stereochemical activity of the $6s^2$ lone pair of Pb^{2+} (or Bi^{3+}), which tends to accommodate itself into an anion site, hence favoring the pyrochlore crystal-structure [21,22]. To suppress the formation of this undesired phase, various methods have been proposed [23,24], the most effective of which uses magnesiumniobate $MgNb_2O_6$ (columbite) as a starting material. Columbite has an octahedral structure similar to that found in the perovskite structure and favors the formation of the PMN–PT phase at a lower temperature. While fine and highly dispersed $MgNb_2O_6$ and TiO_2 raw powders are

*Corresponding authors.
E-mail addresses: gaume@ucf.edu, shi.chen@ucf.edu (S. Chen).

http://dx.doi.org/10.1016/j.ceramint.2014.09.001
0272-8842/

now commercially available, PbO powders are only available in micron size and acicular shapes, which we have found unsuitable for proper densification of high-quality optical ceramics.

During the past few years, several methods have been explored to fabricate lead oxide nanoparticles using direct chemical synthesis [25], sonochemical [26] and sol–gel pyrolysis methods [4]. Among the available processes, the combustion technique is capable of producing ultrafine and uniform powders (less than 100 nm), which help reduce the sintering temperature of ceramics [27–30]. The powder characteristics are dependent on the flame temperature generated during the combustion, which in turn is a function of the nature of fuel and of the fuel-to-oxidant ratio. The effects of different fuels and fuel-to-oxidant ratios on the crystallographic phases produced and powder characteristics have been extensively investigated by Chavan and Tyagi [31] and Bedekar et al. [32] for many oxides. It was established that a careful control of the fuel-to-oxidant ratio is necessary to get the desired product [33]. The choice of a given fuel is essentially determined by its ability to chelate metallic ions in solution. In particular, the amino-acid glycine, with its carboxylic acid function and amino group is a powerful complexing agent for a number of metallic ions [34] and has successfully been used in combination to nitrates to synthesize complex chromites [35], manganites [36], zirconates, ferrites [37,38], and oxide ceramics powders [39]. Similarly, combustion synthesis methods based on carboxylate azides or urea have also been successfully developed for the preparation of oxide ceramic powders such as Fe_2O_3 and Al_2O_3 [40–42]. In this paper, we describe the synthesis of lead oxide nanopowders by the glycine–nitrate process (GNP), for the fabrication of PMN–PT transparent ceramics by solid-state sintering.

2. Experimental

In the combustion process, lead acetate trihydrate (99.999%, Aldrich) and nitric acid (70%, Aldrich) were used as the cation source and oxidant respectively, glycine ($\geq$99%, Aldrich) was used as a fuel (reductive agent). Based on preliminary experiments, we investigated five different glycine-to-nitrate molar ratios, 0.2, 0.5, 0.9, 1.3, 1.7. The required amount of $Pb(CH_3COO)_2 \cdot 3H_2O$ was dissolved in a quartz crucible with 50 ml of water. Different solutions corresponding to the above-mentioned glycine-to-nitrate ratios were prepared and stirred for 20 min and then heated on a hot-plate in a hood. Flame temperatures were measured by a two-color optical pyrometer (Ircon, UX 70P) focused on the glowing ash during combustion. After combustion, the powders were calcined at 420 °C in oxygen atmosphere for 4 h and X-ray diffraction (XRD) (Rigaku, D/Max) was used to evaluate the crystalline phases. The morphology of the powders after ball-milling was examined by scanning electron microscopy (SEM) (Zeiss, Ultra-55). These powders were then subsequently used to prepare PMN–PT ceramics with composition 0.75Pb ($Mg_{1/3}Nb_{2/3}$) $O_3-0.25PbTiO_3$ doped with 3 at% lanthanum, using magnesium niobate ($MgNb_2O_6$, H. C. Starck), titanium oxide ($\geq$99.5%, Aldrich) and lanthanum oxide (99.99%, Alfa Aesar) starting powders. These powders were ball-milled for 20 h and pressed into pellets followed by cold-isostatic pressing (CIP) at 200 MPa.

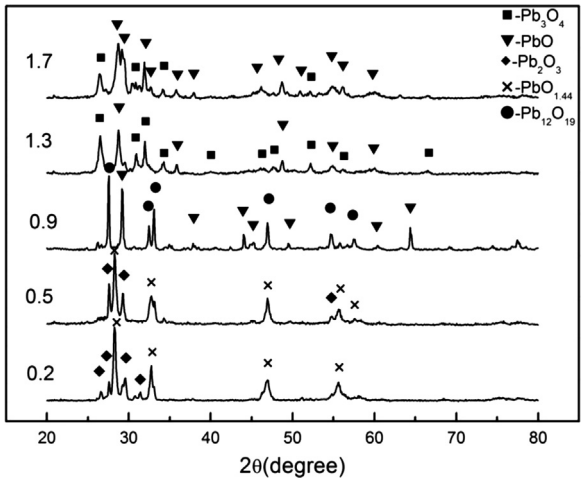

Fig. 1. Powder X-ray diffraction of as prepared ash for different glycine-to-nitrate ratios. (92 × 120 mm (300 × 300 DPI)).

Table 2
Quantitative analysis the powders with different glycine-to-nitrate ratios.

Glycine/Nitrate	Ash composition	Yield (lead load) (%)
1.3	41%PbO+59%Pb_3O_4	73.4
1.7	73%PbO+27%Pb_3O_4	85.6

Table 1
Effect of the glycine-to-nitrate ratio on powder yield.

Glycine: Nitrate	Reaction temperature (°C)	Ash composition	Weight of ash (g)	Weight of ash after calcination (g)	Ratio of weight after and before calcination (%)
0.2	640 ± 15	$Pb_2O_3+PbO_{1.44}$	0.78	0.70	90
0.5	740 ± 25	$Pb_2O_3+PbO_{1.44}$	0.30	0.27	90
0.9	/	$PbO+Pb_{12}O_{19}$	0.15	0.14	93
1.3	600 ± 10	$PbO+Pb_3O_4$	2.35	2.14	91
1.7	590 ± 20	$PbO+Pb_3O_4$	2.60	2.55	98

(*Note*: The theoretical yield should be 3 g in Pb_3O_4 phase. A very quick reaction was observed in the glycine-to-nitrate ratio 0.9, and an equilibrium temperature could not be measured with sufficient accuracy. The spread in the temperature values was obtained by repeating each experiments three times and is not an indication of the pyrometer measurement accuracy. Nanopowders of phase pure Pb_3O_4, showing no measurable coarsening, are obtained after a second calcination at 420 °C in oxygen for 2 h.)

Thermo-Mechanical Analysis (TMA) (Setaram, Dilatometry-System evolution) was used to compare the densification rates of green-bodies prepared with combustion-synthesized lead oxide. Transparent ceramics of PMN–PT were prepared by sintering green-bodies in a tube furnace at 800 °C and for 4 h followed by a dwell at 1150 °C for 4 h in an oxygen atmosphere.

3. Results and discussion

3.1. Effect of glycine-to-nitrate ratio on the formation of lead oxide powders

Upon heating, the auto-ignition of the lead acetate, glycine and nitric acid solution results in the formation of a voluminous ash. In order to fabricate stoichiometric PMN–PT ceramics with these lead oxide precursor, it is essential to know the proper stoichiometry of the lead oxide produced. Hence, after combustion-synthesis, the powders were calcined at 420 °C in an oxygen atmosphere for 4 h in an attempt to shift the valence state of lead to Pb^{2+}. This facilitates Table 1 shows the reaction temperature during combustion as a function of the glycine-to-nitrate ratio. The reaction temperature goes through a maximum as the glycine-to-nitrate ratio increases (Table 1). When nitric acid and glycine are in stoichiometric proportions, the reaction temperature is the highest. We observe that the weight of collected ash decreases as the reaction temperature increases. This can be simply explained by the fact that volatilization of the reactants is more pronounced at high temperatures. The weight loss after calcination is within 10%. Fig. 1 shows the X-ray diffraction of the produced lead oxide after calcinations and for different glycine-to-nitrate ratios. From the XRD data, we were able to determine the phases and composition of the different calcined ashes (Table 1). According to Chick et al. [39], for glycine–nitrate combustion, N_2, CO_2 and H_2O are primarily evolved as gaseous products. The complexity of the redox reactions involved during the combustion in such an open system may however limit our ability to draw a direct correlation between the G/N ratio and the nature of the solid phases obtained. In the subsequent analysis, we only consider powders obtained with 1.3 and 1.7 G/N ratios because the powder yields are much larger than those achieved with other ratios. Table 2 summarizes the results of quantitative X-ray diffraction analysis

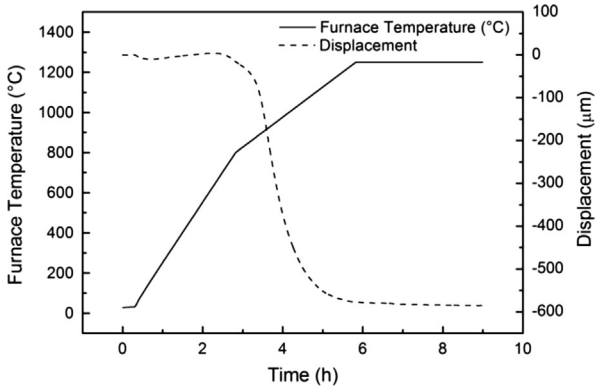

Fig. 3. TMA of a PMN–PT green body made from combustion-synthesized lead oxide nanopowders. (84 × 120 mm^2 (300 × 300 DPI)).

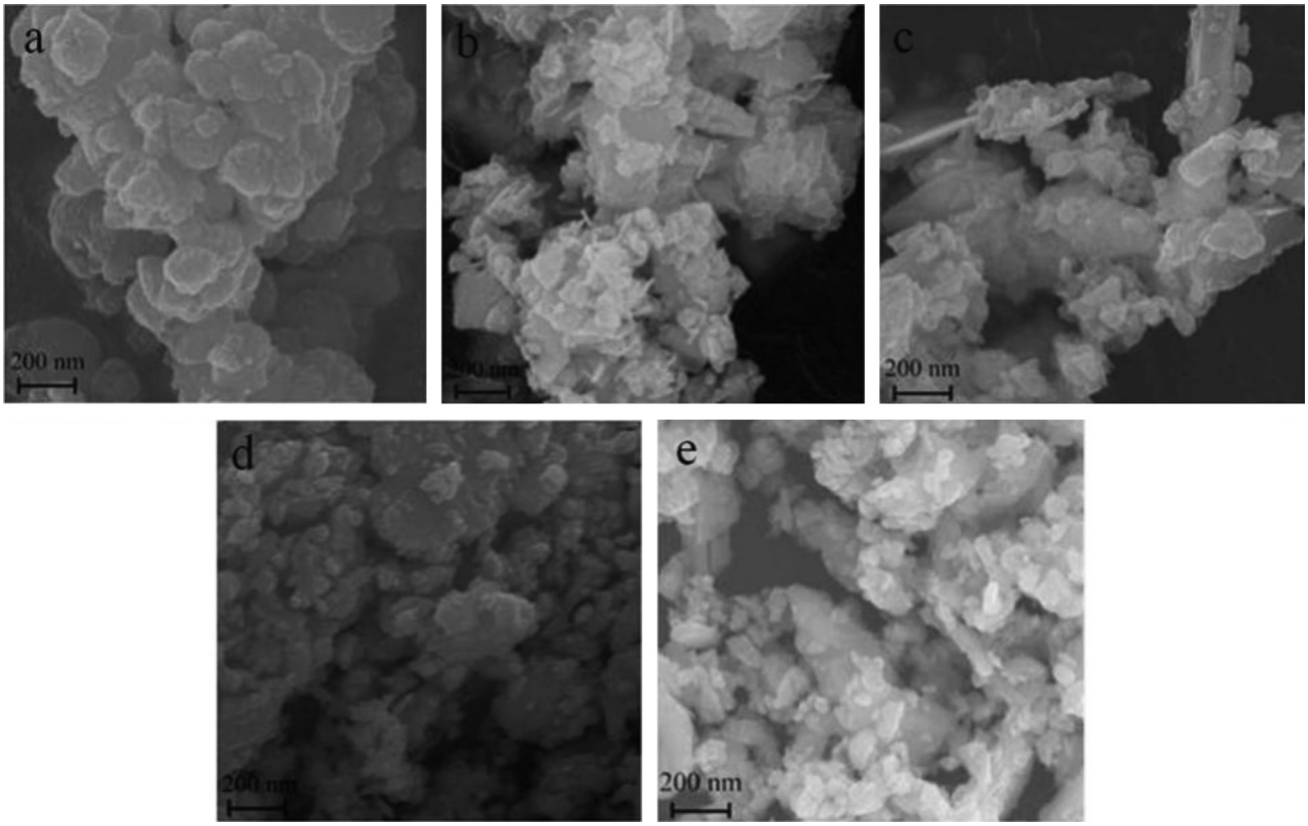

Fig. 2. SEM photographs of powders obtained with different glycine-to-nitrate ratios (a) 0.2; (b) 0.5; (c) 0.9; (d) 1.3; (e) 1.7. (76 × 120 mm^2 (300 × 300 DPI)).

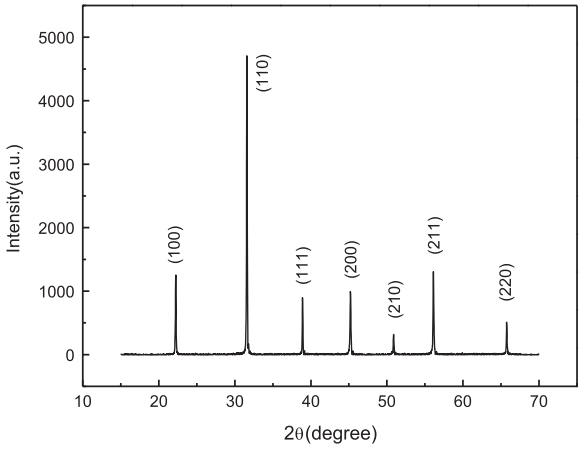

Fig. 4. XRD on a PMN–PT ceramic made from combustion-synthesized lead oxide nanopowders. (92 × 120 mm^2 (300 × 300 DPI)).

carried on these two powders. For a glycine-to-nitrate ratio of 1.7, a maximum yield of 85.6% in lead is obtained. Fig. 2 shows the SEM photographs of lead oxide powders produced by combustion synthesis with 0.2, 0.5, 0.9, 1.3 and 1.7 glycine-to-nitrate molar ratios and after ball-milling. After combustion, the as-produced particles are agglomerated. The morphology of the particles vary from platelet-like at low G/N values (< 0.9) whereas for higher G/N ratios, the primary particles are spherical with an average size of 60 nm.

3.2. Solid-state synthesis of PMN–PT transparent ceramics

Based on the previous results, we selected lead oxide nanopowders synthesized with a 1.7 glycine-to-nitrate ratio for the fabrication of PMN–PT transparent ceramics of composition 0.75Pb $(Mg_{1/3}Nb_{2/3})O_3 - 0.25PbTiO_3$ doped with

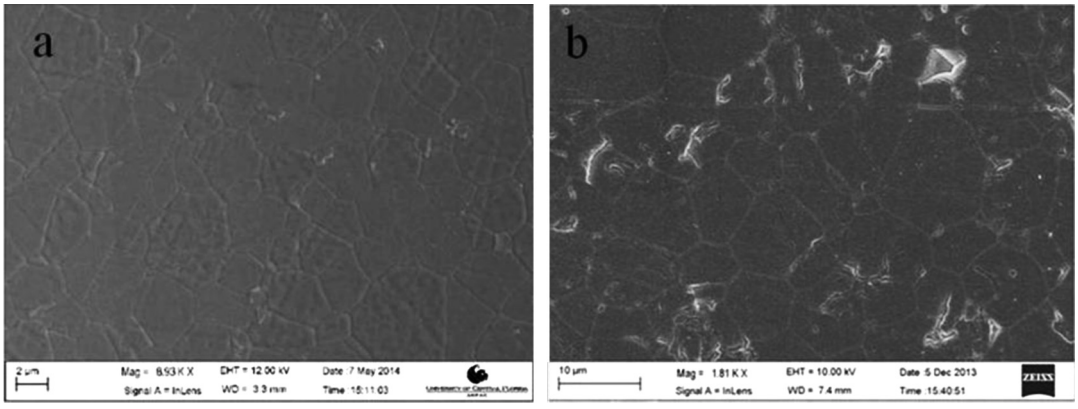

Fig. 5. SEM photographs of PMN–PT ceramics made from (a) combustion-synthesized lead oxide; (b) commercial lead oxide. (45 × 120 mm^2 (300 × 300 DPI)).

Fig. 6. Photographs of PMN–PT ceramics made from (a and b) combustion-synthesized lead oxide nanopowders; (c and d) and from commercial lead oxide. (92 × 120 mm^2 (300 × 300 DPI)).

3 at% La. The densification of the PMN–PT green-bodies was measured by the thermomechanical analysis (TMA). Fig. 3. shows that the densification and densification rate of a PMN–PT green body made with combustion-synthesized lead oxide powders. We found that the densification is three times higher than that of a PMN–PT green body made with commercial lead oxide powders. After reactive sintering, XRD on the ceramic shows a pure perovskite phase devoid of pyrochlore (Fig. 4). Fig. 5 compares the microstructures of sintered ceramics made with combustion synthesized lead oxide and commercial lead oxide. The samples were polished with an alumina suspension and thermally-etched at 800 °C for 30 min. In the case of the ceramic made with combustion-synthesized lead oxide, the grain-size is smaller (3 μm) than that of a ceramic made with commercial lead oxide (9 μm). The former is also fully dense while the latter still has some intergranular and intragranular porosity, which turns out to be detrimental to the transparency of the ceramic as can be seen on Fig. 6.

4. Conclusion

A glycine–nitrate combustion synthesis can be used to fabricate lead oxide with small particle size. It is found that the glycine-to-nitrate ratio affects the phase formation, valence, yield and shape of the lead oxide powders. When the amount of nitric acid (oxidant agent) and glycine (reductive agent) are in stoichiometric proportions, the reaction temperature is at its highest. However because of volatile loss, the ash yield decreases as the reaction temperature increases. Lead oxide powders synthesized by this method have smaller particle size than commercial powders, and help improving the densification of green-bodies and the transparency of PMN–PT ceramics.

Acknowledgments

The authors would like to thank the Israeli Ministry of Defense for support through contract # 100254098.

References

[1] A. Thulasiromudu, S. Buddhudu, Optical characterization of Eu^{3+} and Tb^{3+} ions doped zinc lead borate glasses, Spectrochim. Acta-A 66 (2007) 323–328.
[2] K. Konstantinov, S.H. Ng, J.Z. Wang, G.X. Wang, D. Wexler, H.K. Liu, Nanostructured PbO materials obtained in situ by spray solution technique for Li-ion batteries, J. Power Sour. 159 (2006) 241–244.
[3] C. Barriga, S. Maffi, L.P. Bicelli, C. Malitesta, Electrochemical lithiation of Pb_3O_4, J. Power Sour. 34 (1991) 353–358.
[4] H. Karami, M. Ghamooshi-Ramandi, Synthesis of sub-micro and nanometer sized lead oxide by sol–gel pyrrolysis method and its application as cathode and anode of lead-acid batteries, Int. J. Electrochem. Sci. 8 (2013) 7553–7564.
[5] M. Veithen, X. Gonze, P. Ghosez, First-principles study of the electro-optic effect in ferroelectric oxides, Phys. Rev. Lett. 93 (2004) 187401–187404.
[6] K. Uchino, Electro-optic ceramics and their display applications, Ceram. Int. 21 (1995) 309–315.
[7] L.S. Kamzina, R. Wei, G. Li, J. Zeng, A. Ding, Electro-optical properties of PMN–xPT compounds: single crystals and transparent ferroelectric ceramics, Phys. Solid State 52 (2010) 2142–2146.
[8] H. Fu, R.E. Cohen, Polarization rotation mechanism for ultrahigh electromechanical response in single-crystal piezoelectrics, Nature 403 (2000) 281–283.
[9] A.A. Gültekin, H. Yilmaz, Processing and electrical properties of $(1-x)[(1-y)(Pb(Mg_{1/3}Nb_{2/3})O_3)-y(Pb(Yb_{1/2}Nb_{1/2})O_3)]-xPbTiO_3$ ceramics, Mater. Lett. 63 (2009) 584–586.
[10] Z.H. Wei, T. Tsuboi, Y. Nakai, Y.L. Huang, J.T. Zeng, G.R. Li, The synthesis of Er^{3+}-doped PMN–PT transparent ceramic and its infrared luminescence, Mater. Lett. 68 (2012) 57–59.
[11] G.H. Haertling, Ferroelectric ceramics: history and Technology, J. Am. Ceram. Soc. 82 (1999) 797–818.
[12] J.G. Baek, T. Isobe, M. Senna, Synthesis of pyrochlore free $0.9Pb(Mg_{1/3}Nb_{2/3})O_3-0.1PbTiO_3$ ceramics via a soft mechanochemical route, J. Am. Ceram. Soc. 80 (1997) 973–981.
[13] P. Ravindranathan, S. Komareni, A.S. Bhalla, R. Roy, Synthesis and dielectric properties of sol–gel derived $0.9Pb(Mg_{1/3}Nb_{2/3})O_3-0.1PbTiO_3$ ceramics, J. Am. Ceram. Soc. 74 (1991) 2996–2999.
[14] A.D. Sheikh, H.H. Kumar, V.L. Mathe, Dielectric properties of chemically co-precipitated tetragonal $Pb(Mg_{1/3}Nb_{2/3})_{0.65}Ti_{0.35}O_3$, Solid State Sci. 12 (2010) 1534–1539.
[15] D.H. Suh, D.H. Lee, N.K. Kim, Phase developments and dielectric/ferroelectric response in the PMN–PT system, J. Eur. Ceram. Soc. 22 (2002) 219–223.
[16] S.M. Gupta, P.R. Bedekar, A.R. Kulkarni, Synthesis, dielectric and microstructure studies of lead magnesium niobate stabilized using lead titanate, Ferroelectrics 189 (1996) 17–25.
[17] J.P. Guha, D.J. Hong, H.U. Anderson, Effect of excess PbO on the sintering characteristics and dielectric properties of Pb $(Mg_{1/3}Nb_{2/3})O_3$–$PbTiO_3$-based ceramics, J. Am. Ceram. Soc. 71 (1988) 152–154.
[18] J. Kelly, M. Leonard, C. Tantigate, A. Safari, Effect of composition on the electromechanical properties of $(1-x)Pb(Mg_{1/3}Nb_{2/3})O_3-xPbTiO_3$, J. Am. Ceram. Soc. 80 (1997) 957–964.
[19] M. Ghasemifard, S.M. Hosseini, Gh.H. Khorrami, Synthesis and structure of PMN–PT ceramic nanopowder free from pyrochlore phase, Ceram. Int. 35 (2009) 2899–2905.
[20] H. Jiang, Y.K. Zou, Q. Chen, K.K. Li, R. Zhang, Y. Wang, Transparent electro-optic ceramics and devices, Inter. Soc. Optical Eng. 5644 (2005) 380–394.
[21] C. Cascales, I. Rasines, P. Garcia Casado, J. Vega, The new pyrochlores $Pb_2(M_{0.5}Sb_{1.5})O_{6.5}$ (M = Al, Sc, Cr, Fe, Ga, Rh), Mater. Res. Bull. 20 (1985) 1359–1365.
[22] N. Wakiya, A. Saiki, N. Ishizawa, K. Shinozaki, N. Mizutani, Crystal growth, crystal structure and chemical composition of a pyrochlore type compound in lead–magnesium–niobium–oxygen system, Mater. Res. Bull. 28 (1993) 137–143.
[23] M. Lejeune, J.P. Boilot, Influence of ceramic processing on dielectric properties of perovskite type compound: $Pb(Mg_{1/3}Nb_{2/3})O_3$, Ceram. Int. 9 (1983) 119–122.
[24] H.C. Wang, W.A. Schulze, The role of excess magnesium oxide or lead oxide in determining the microstructure and properties of lead magnesium niobate, J. Am. Ceram. Soc. 73 (1990) 825–832.
[25] M. Alagar, T. Theivasanthi, A.K. Raja, Chemical synthesis of nano-sized particles of lead oxide and their characterization studies, J. Appl. Sci. 12 (2012) 398–401.
[26] H. Karami, M.A. Karimi, S. Haghdar, A. Sadeghi, R. Mir-Ghasemi, S. Mahdi-Khani, Synthesis of lead oxide nanoparticles by Sonochemical method and its application as cathode and anode of lead-acid batteries, Mater. Chem. Phys. 108 (2008) 337–344.
[27] N.M. Sammes, Z. Cai, Ionic conductivity of ceria/yttria stabilized zirconia electrolyte materials, Solid State Ion. 100 (1997) 39–44.
[28] W. Huang, P. Shuk, M. Greenblattt, Properties of sol–gel prepared $Ce_{1-x}Sm_xO_{2-x/2}$ solid electrolyte, Solid State Ion. 100 (1997) 23–27.
[29] M. Yoshimura, W. Suchanek, In situ fabrication of morphology-controlled advanced ceramic materials by soft solution processing, Solid State Ion. 98 (1997) 197–208.

[30] S.V. Chavan, A.K. Tyagi, Combustion synthesis of nanocrystalline yttria-doped ceria, J. Mater. Res. 19 (2004) 474–480.
[31] S.V. Chavan, A.K. Tyagi, Preparation and characterization of $Sr_{0.09}Ce_{0.91}O_{1.91}$, $SrCeO_3$, and Sr_2CeO_4 by glycine-nitrate combustion: crucial role of oxidant-to-fuel ratio, J. Mater. Res. 19 (2004) 3181–3188.
[32] V. Bedekar, S.V. Chavan, A.K. Tyagi, Highly sinter-active nanocrystalline RE_2O_3 (RE=Gd, Eu, Dy) by a combustion process, and role of oxidant-to-fuel ratio in preparing their different crystallographic modifications, J. Mater. Res. 22 (2007) 587–594.
[33] G. Singh, V.S. Tiwari, P. Tiwari, A.K. Srivastava, P.K. Gupta, Effect of oxidant-to-fuel ratios on phase formation of PLZT powder; prepared by gel-combustion, J. Alloys Compd. 509 (2011) 4127–4231.
[34] P. Ravindranathan, K.C. Patil, A one-step process for the preparation of γ-Fe_2O_3, J. Mater. Sci. Lett. 5 (1986) 221–222.
[35] Y.J. Yang, T.L. Wen, H.Y. Tu, D.Q. Wang, J.H. Yang, Characteristics of lanthanum strontium chromite prepared by glycine nitrate process, Solid State Ion. 135 (2000) 475–479.
[36] A. Alqat, Z. Gebrel, V. Kusigerski, V. Spasojevic, M. Mihalik, J. Blanusa, Synthesis of hexagonal $YMnO_3$ from precursor obtained by the glycine–nitrate process, Ceram. Int. 39 (2013) 3183–3188.
[37] H. Mohseni, H. Shokrollahi, I. Sharifi, K. Gheisari, Magnetic and structural studies of the Mn-doped Mg–Zn ferrite nanoparticles synthesized by the glycine nitrate process, J. Magn. Magn. Mater. 324 (2012) 3741–3747.
[38] N. Kikukawa, M. Takemori, Y. Nagano, M. Sugasawa, S. Kobayashi, Synthesis and magnetic properties of nanostructured spinel ferrites using a glycine–nitrate process, J. Magn. Magn. Mater. 284 (2004) 206–214.
[39] L.A. Chick, L.R. Pederson, G.D. Maupin, J.L. Bates, L.E. Thomas, G.J. Exarhos, Glycine–nitrate combustion synthesis of oxide ceramic powders, Mater. Lett. 10 (1990) 6–12.
[40] P. Ravindranathan, K.C. Patil, A low temperature path to the preparation of ultrafine ferrites, Am. Ceram. Soc. Bull. 66 (1987) 668–692.
[41] P. Ravindranathan, G.V. Mahesh, K.C. Patil, Low-temperature preparation of fine-particle cobaltites, J. Solid State Chem. 66 (1987) 20–25.
[42] J.J. Kingsley, K.C. Patil, A novel combustion process for the synthesis of fine particle α-alumina and related oxide materials, Mater. Lett. 6 (1988) 427–432.